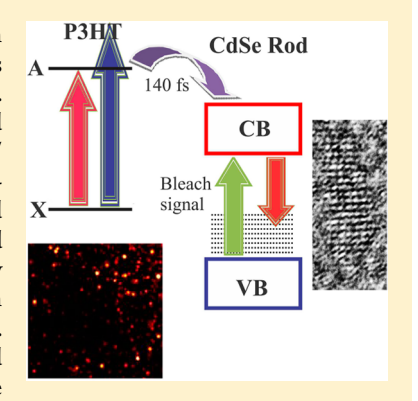
# Investigation of Fluorescence Emission from CdSe Nanorods in PMMA and P3HT/PMMA Films

Lorinc Sarkany, † Jenna M. Wasylenko, ‡ Santanu Roy, † Daniel A. Higgins, \*, † Christopher G. Elles, \*, ‡ and Viktor Chikan\*,†

Supporting Information

**ABSTRACT:** Complementary fluorescence microscopy and ultrafast transient absorption spectroscopy measurements spanning a range of time scales from seconds to femtoseconds probe the interfacial dynamics of charge carriers in CdSe nanorod/polymer blends. Together, these very different techniques provide new information about the origin and dynamics of below-band-edge emission from CdSe nanorods in CdSe/PMMA and CdSe/ P3HT/PMMA films [PMMA = poly(methyl methacrylate); P3HT = poly(3hexylthiophene)]. Emission below the band edge of the CdSe nanorods is associated with surface defects (traps) at the nanoparticle/polymer interface, where conduction band electrons radiatively relax to the intraband defect sites. The fluorescence microscopy experiments simultaneously monitor both the trap emission and the band edge emission from single nanoparticles, and reveal that the two emission channels are distinct. Transitions between the two emissive states occur on time scales longer than ~20 ms, and always involve an intermediate dark state in which no emission is observed. The presence



of P3HT increases the relative band edge emission intensity and reduces the fluorescence intermittency (blinking) of both emissive states. The ultrafast transient absorption experiments monitor the evolution of a stimulated emission band below the CdSe band edge following excitation of P3HT. The measurements reveal ultrafast electron transfer from photoexcited P3HT to the CdSe nanorods within the instrument response time of approximately 140 fs, and confirm that there is strong coupling between the nanorods and P3HT in these dilute blends. Analysis of separate CdSe nanorod etching experiments suggests that the trap states are formed by the removal of atoms from the ends of the nanorods in the presence of chloroform. Mechanisms for charge trapping at the nanoparticle/polymer interface are discussed.

# ■ INTRODUCTION

The development of novel photovoltaic devices for solar energy conversion requires photoactive materials that are efficient, durable, and easy to manufacture. Many of the most promising new materials that meet these requirements are hybrid systems consisting of inorganic nanostructures embedded in conductive polymer matrices. 1-5 For example, functional solar cells have been prepared from CdSe quantum dots, rods, and tetrapods dispersed in the conductive polymer poly(3-hexylthiophene) (P3HT).5 Hybrid CdSe/P3HT materials are good candidates for tandem solar cells that capture light in two stages because CdSe has a relatively large band gap and efficiently captures light from the blue part of the solar spectrum. The best CdSe/ polymer solar cells produced to date have efficiencies reaching 2.6-2.8%, depending on the structure of the nanoparticle. Nonspherical nanostructures are promising in these types of solar cells because higher packing efficiency can be achieved. In addition, due to reduced Auger recombination rates, elongated nanostructures exhibit longer excitonic lifetimes for improved power conversion efficiencies.7 Among other factors, the surface quality of the nanoparticles<sup>8</sup> and the interaction of the coating ligands with the matrix<sup>9</sup> determine the overall efficiency and durability of these materials. Further improvement of hybrid inorganic/organic solar cell materials therefore requires a better understanding of the fundamental details of charge separation and migration across the interface, as well as possible chemical changes that occur following the absorption of light.

One way to study the underlying processes that inhibit solar energy conversion in hybrid nanoparticle/polymer materials is to observe the nanoparticle fluorescence. Fluorescence measurements monitor the charge carrier dynamics, including charge trapping and recombination. The emission of light occurs upon radiative recombination of an electron and a hole. Therefore, the fluorescence intensity of a material is proportional to the number of radiatively recombining electron-hole pairs and the emission wavelength reports on their relative energies. Fluorescence intermittency (or blinking) measurements reveal charge trapping and other processes that potentially inhibit energy conversion by blocking the formation and transport of new charge carriers, 10-14 whereas time-

Received: May 8, 2013 Revised: August 21, 2013 Published: August 21, 2013

<sup>&</sup>lt;sup>†</sup>Department of Chemistry, Kansas State University, Manhattan, Kansas 66506-3701, United States

<sup>\*</sup>Department of Chemistry, University of Kansas, Lawrence, Kansas 66045-7572, United States

resolved fluorescence decay measurements provide information about the kinetics of the excited system.

The fluorescence intermittency, or blinking behavior, of CdSe semiconductor nanoparticles has been of interest in the scientific community over the past decade. 10-14 In blinking measurements, the nanoparticles are observed to switch between fluorescent (ON) and nonfluorescent (OFF) states, where the ON and OFF times follow a power law distribution.<sup>14</sup> Experiments and theory indicate that blinking may be a result of charge trapping that temporarily leaves the nanoparticle in a charged state, thus preventing further excitation and/or emission. <sup>15,16</sup> In this charging model, the photoluminescence quantum yield correlates well with shorter emission lifetimes. A second model that was recently discussed by Galland et al. 17 shows that blinking could also be the result of fluctuations in the electron accepting surface sites. In this type of blinking, the change in photoluminescence quantum yield is not followed by significant changes in the recombination dynamics. The immediate surroundings of the luminescent nanoparticle is clearly important in determining whether the charge will migrate into the matrix or remain confined in close proximity to the nanostructure. 18 Because charge trapping generally occurs at the interface, various methods have been used to minimize trapping effects by protecting the surface of the nanoparticle. For example, growing a shell of large-bandgap semiconductor around the CdSe nanoparticle has been shown to suppress surface traps and improve the overall emission quantum yield, 19 although tunneling to the surrounding matrix can still play a role in charge trapping. 15 Jha and Guyot-Sionnest 20 have shown that not only charge tunneling, but also strong confinement of excitons leads to increased recombination rates. Recently, Jander et al.<sup>21</sup> found that the intermittency of CdSe nanorod emission was suppressed when the nanorods were located near an amorphous carbon layer due to Forster-type energy transfer that efficiently competes with charge transfer to trap sites. Similar to the work by Jander et al., some of us<sup>22</sup> observed longer ON times and increased fluorescence intensity for CdSe nanorods in the presence of the conductive polymer P3HT. The increased fluorescence of CdSe nanorods in the presence of P3HT was attributed to a filling of surface traps via static charge transfer from the conductive polymer.<sup>22</sup>

Understanding interfacial charge carrier dynamics at and across the CdSe/polymer boundary requires further investigation of the nanoparticle emission properties. In addition to band edge emission, where conduction band electrons recombine with valence band holes, trap state emission has also been discussed in the literature. <sup>23,24</sup> Trap state emission below the band edge energy can be attributed to the radiative recombination of trapped electrons with valence band holes, conduction band electrons with trapped holes, or trapped electrons with trapped holes. The electron and hole traps are defects that lie energetically between the valence band and conduction band. Emission from conduction band electrons recombining with hole traps and from trapped electrons recombining with valence band holes have both been observed, depending on the relative composition of the nanoparticle surface. 23,24 For example, some of us recently observed relatively strong emission below the band edge for CdSe nanorods dispersed in a poly(methyl methacrylate) (PMMA) polymer matrix.<sup>22</sup> This relatively strong trap emission from the CdSe nanorods was attributed to radiative recombination of conduction band electrons with trapped holes (defect sites)

lying above the valence band. Importantly, the addition of dilute P3HT enhanced the relative band edge emission of the CdSe nanorods by filling the intraband defects of CdSe with electrons via charge transfer from the P3HT. <sup>22</sup>

In this paper, we present complementary single particle fluorescence intermittency and ultrafast transient absorption measurements that provide deeper insight into the interfacial dynamics and charge trapping behavior of CdSe nanoparticles. Specifically, we probe the interaction between bare, uncoated CdSe nanorods and dilute P3HT dispersed in PMMA (CdSe/ P3HT/PMMA) by monitoring the band edge and trap emission of the nanoparticles. New single-point fluorescence intermittency measurements presented here support a threestate model for fluorescence blinking that includes distinct band edge emission, trap emission, and dark (OFF) states. Here, band edge emission refers to fluorescence at the band edge energy of CdSe nanoparticles, whereas "trap emission" describes radiative relaxation of a conduction band electron to a localized defect (trap) located above the valence band of CdSe.<sup>25</sup> We show that the trap emission and band edge emission are negatively correlated, indicating that the three states of the nanoparticle are distinct, and that the switching among these emissive and dark states occurs on a milliseconds to seconds time scale under continuous irradiation. Complementary femtosecond transient absorption measurements probe the interfacial charge transfer and ultrafast recombination dynamics by monitoring the stimulated emission of CdSe nanorods following optical excitation of P3HT. The ultrafast measurements confirm that there is efficient charge transfer from P3HT to CdSe upon photoexcitation of the conductive polymer and verify the nature of the trap emission in the microscopy experiments. Finally, we explore the role of photochemical etching in creating new surface trap sites, and comment on the chemical composition of the traps. Collectively, these experiments provide a detailed view of the interfacial dynamics and charge trapping behavior of CdSe nanorods in an environment that closely resembles functional hybrid nanoparticle/polymer solar cell materials.

# ■ EXPERIMENTAL METHODS

Synthesis of CdSe Nanorods. CdSe nanorods were synthesized under oxygen-free conditions. 16 The reaction mixture, comprising 50 mg of CdO, 4.1 g of trioctylphosphine oxide (TOPO), and 305 mg of tetradecylphosphonic acid (TDPA), was prepared in a three-neck flask with septum, a thermometer, and a refluxing column. The refluxing column was attached to a Schlenk line. The solution was first heated to 120 °C under argon flow and subsequently placed under vacuum for 1 h. A selenium-trioctylphosphine (SeTOP) solution was prepared separately in a nitrogen-filled glovebox. A mixture of 4 mL of trioctylphosphine (TOP) and 42 mg of Se powder were placed into a vial that was then capped with a septum. The solution was stirred in the glovebox with a magnetic stirrer. The Se dissolved in TOP in ~0.5 h. The solution temperature was then raised to 280 °C, after which it became golden yellow. At this point, the cadmium solution was returned to atmospheric pressure and the temperature was increased to 270 °C. The SeTOP solution was then injected and the solution temperature decreased to 230  $^{\circ}\text{C}.$  Growth of the nanorods was performed at 260  $^{\circ}\text{C}.$  The entire growth process was monitored by UV-visible and photoluminescence spectroscopy. Nanorod growth was terminated after ~5 min. Methanol was added to the reaction mixture once the solution

had cooled to room temperature. The mixture was then centrifuged and the supernatant was discarded. This process was repeated five times. A dark red solution was obtained when the nanorods were dissolved in spectroscopic grade toluene. The crude reaction mixture was washed thoroughly with methanol to remove the phosphine ligands. The binding strength of the ligands is sufficiently low that they are easily removed by washing with organic solvents. <sup>26</sup>

**Etching of CdSe Nanorods.** The etching of the CdSe nanorods was performed in a temperature controlled fiber optic fluorescence setup. A diode laser of wavelength 405 nm and 6.5 mW power was used to irradiate the sample continuously. The solutions were placed in quartz fluorescence cuvettes and were heated at 40 °C for 72 h with continuous stirring. Photoluminescence spectra were recorded at five minute intervals, but only the photoluminescence spectra recorded at room temperature before and after heat treatment are presented here.

**Film Preparation.** Two different types of films containing the CdSe nanorods were prepared. The first was a CdSe/ PMMA composite, and the second was a CdSe/P3HT/PMMA composite where the nanorods were dispersed in a PMMA film doped with dilute P3HT. PMMA (MW = 120 000 g/mol) was obtained from Sigma-Aldrich and was used as received. P3HT (regionegular form, MW = 20000-70000) was obtained from American Dye Source and was also used as received. Two separate PMMA solutions were prepared by dissolving 0.05 g of PMMA in 2 mL of chloroform. To the first PMMA solution, 2 mL of nanorods in toluene was added and mixed well. A solution of P3HT was prepared by dissolving 0.003 g of P3HT in 4 mL of chloroform. A 0.04 mL aliquot of this P3HT solution was then added to the second PMMA solution, yielding a 6% (by weight) mixture of P3HT in PMMA. A 2 mL aliquot of nanorods in toluene was then added to the PMMA/ P3HT mixture and mixed well. The CdSe/PMMA and CdSe/ P3HT/PMMA films were obtained by spin-casting (1500 rpm, 1 min) a single drop of the appropriate solution onto a glass coverslip (FisherFinest). Film thickness was determined on a spectroscopic ellipsometer (J. A. Woolam,  $\alpha$ -SE). Average thicknesses of the CdSe/PMMA and CdSe/P3HT/PMMA composite films were 49  $\pm$  23 and 53  $\pm$  32 nm, respectively.

Confocal Microscopy. Single point fluorescence time transients were acquired over several hundred seconds, under continuous illumination, using a sample-scanning confocal microscope that has been described previously.<sup>27</sup> Briefly, this system is built upon an inverted epi-illumination microscope (Nikon TE-300). The composite films were placed on top of a closed-loop piezoelectric x,y-scanning stage (Sifam Instruments) attached to this microscope. A diode laser (Spectra-Physics, Cyan Scientific, 488 nm) was used as the excitation source. The laser light was directed into the epi-illumination port of the microscope and reflected from a dichroic beam splitter (Chroma, 505 DCLP) into the back aperture of an oil immersion objective (Nikon Plan Fluor, 100× magnification, 1.3 numerical aperture (NA)). The fluorescence was collected with the same objective and passed back through the dichroic beam splitter and subsequently through a holographic notch filter. The band edge and trap emission were separated by directing the fluorescence onto a 700 nm dichroic short-pass filter (Chroma E700sp). The reflected trap emission was further filtered with a 700 nm long-pass filter, while the transmitted band edge emission was directed through a 580 nm band-pass filter with 40 nm bandwidth. The band edge and trap emission were detected simultaneously, using separate single

photon counting avalanche photodiodes. Fluorescence images were acquired by raster scanning the sample above the focused laser spot. Single point fluorescence time transients were collected by recording the spectrally integrated fluorescence in time from selected points in the sample, with 20 ms time resolution.

Statistical analysis of the blinking behavior observed in the time transients was accomplished by first defining separate threshold limits for ON and OFF states in each fluorescence channel. The threshold values were set to twice the standard deviation of the background signal. An emission channel is considered ON when the emission intensity exceeds the threshold for that channel. If both channels are below the respective thresholds, the system is considered to be in the dark OFF state. We observe that the band edge emission, trap emission, and OFF times follow power-law distributions having different exponents. Note that the time scales associated with the power law exponents are better thought of as persistence times and not actual lifetimes of the states. Instances where both channels exceed the threshold are rare, typically less than one percent of the total measurement time, which justifies the use of a three-state model with distinct ON states. However, dual-emission points are included in the statistical analysis, and are assigned to the emissive state (band edge or trap) with the largest signal above threshold.

**Widefield Video Microscopy.** Fluorescence videos were recorded on a widefield microscope. <sup>28</sup> This system is built upon an inverted epi-illumination microscope (Nikon Eclipse Ti). For uniform illumination of the sample, 488 nm laser light was passed through a spinning optical diffuser and then reflected from a dichroic beamsplitter and into the back aperture of an oil immersion objective (Nikon Apo TIRF, 100x, 1.49 N.A.). The incident laser power was maintained in the 1 mW range throughout these experiments. Fluorescence from the sample was collected in reflection and was separated from the excitation light by passage back through the dichroic beamsplitter. The fluorescence was subsequently directed through an image splitter (Cairn Research, Optosplit II) fitted with an appropriate dichroic beamsplitter. The band edge emission was subsequently passed through a 580 nm bandpass filter (40 nm passband) and the trap emission through a 700 nm long-pass filter. The band edge emission and the trap emission were recorded simultaneously on a back-illuminated EM-CCD camera (Andor iXon DU-897). Videos were recorded at a frame rate of  $\sim$ 2 frames per second.

Transient Absorption. Ultrafast transient absorption measurements were performed using a regeneratively amplified Ti:sapphire laser (Legend Elite USP; Coherent) that produces 35 fs pulses of light at a repetition rate of 1 kHz. Nonlinear frequency conversion of the 800-nm laser fundamental in an optical parametric amplifier (TOPAS-C; Light Conversion) generates pump pulses at 630 nm. The pump pulses were attenuated to 0.25  $\mu$ J and gently focused to a spot size of 1 mm at the sample. The attenuated pulses have a duration of about 120 fs. Probe pulses in the range 450-765 nm were obtained by focusing a small amount of the fundamental laser light into a 3 mm sapphire window to produce broadband continuum, which is then collimated and passed through two colored-glass filters to remove the residual 800 nm fundamental and sampledamaging UV radiation, respectively. An off-axis parabolic mirror focuses the probe to a spot size of 0.1 mm at the sample, where it is overlapped with the pump beam. After passing through the sample, an imaging spectrograph disperses the

continuum probe light onto a 256 pixel silicon photodiode array for shot-to-shot detection. The time-dependent transient absorption spectra were obtained by averaging 2000 laser shots at each delay time, with a 500 Hz chopper blocking every other pump pulse for active background subtraction. Transient spectra are dispersion-corrected to account for the wavelength-dependent arrival time of the probe light. The transient absorption measurements use CdSe/PMMA, P3HT/PMMA, and CdSe/P3HT/PMMA samples with the same composition as described above, except that the film thickness was increased to give suitable optical densities for the ultrafast experiments. The laser fluence of  $\sim\!\!30~\mu\mathrm{J/cm^2}$  was well below the reported damage threshold for CdSe nanoparticles.

#### RESULTS AND DISCUSSION

Fluorescence Intermittency. The representative fluorescence microscopy images in Figure 1 show the maximum intensity of band edge and trap emission observed at each pixel for CdSe nanorods dispersed in CdSe/PMMA and CdSe/ P3HT/PMMA films under continuous irradiation at 488 nm. Plotting the data in this manner depicts an image similar to what would be obtained in the absence of nanorod blinking. This wavelength excites both CdSe nanorods and the P3HT polymer, although the emission signal is almost entirely from the nanorods. The strongly localized CdSe emission reveals the locations of the nanorods in each image, whereas the diffuse P3HT emission bleaches within a few seconds and therefore contributes only weakly to the background signal. The early time evolution of the P3HT emission is excluded from the temporal analysis of the confocal microscopy data (below) in order to selectively investigate the behavior of CdSe emission states. The widefield microscopy images in Figure 1 show that both band edge and trap emission are relatively weak for CdSe nanorods dispersed in a PMMA matrix (Figure 1E,F), but that the band edge emission of the nanorods is dramatically enhanced in the presence of dilute P3HT (Figure 1E). Meanwhile the trap emission is only slightly enhanced in the presence of P3HT(Figure 1F). Widefield images recorded under 632 nm excitation yielded little detectable emission from P3HT or the nanorods. The number densities of the CdSe nanorods are very similar in both CdSe/P3HT/PMMA and CdSe/PMMA samples, which indicates that in the P3HT matrix there are many more actively emitting rods.

As shown previously,<sup>22</sup> neither the band edge nor the trap emission signals from these samples are continuous. Rather, they exhibit dramatic fluctuations in time (i.e., fluorescence intermittency, or blinking), as shown in the widefield microscopy videos provided in the Supporting Information. Using a confocal microscope to simultaneously record fluorescence time transients for both the band edge and trap emission channels at single sites in each film provides an unique opportunity to observe the competition between the two emissive states, as well as the blinking statistics of each state. Representative examples of the fluorescence time transients over several hundred seconds are shown in Figure 2.

The right side of Figure 2 shows the single-point emission signals for each detection channel as a function of time for CdSe nanorods in CdSe/PMMA (Figure 2B) and CdSe/P3HT/PMMA (Figure 2C) films. The detector dark counts are also plotted for comparison (top panel). The left half of Figure 2 shows the (log-scale) probability distributions as a function of emission intensity in the band edge and trap emission channels. These 2D color maps demonstrate that the signals in the two

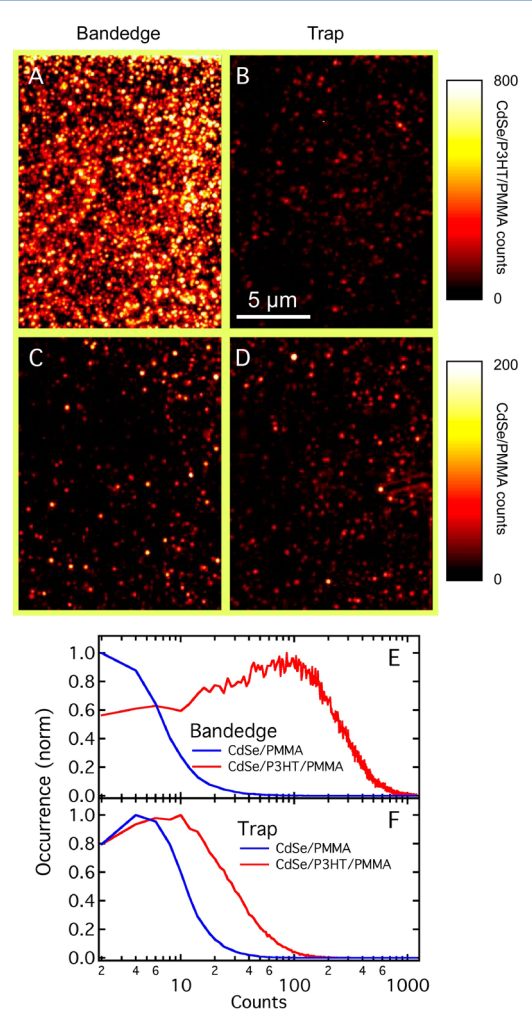


Figure 1. Widefield fluorescence microscopy images of the band edge emission (A and C) and trap emission (B and D) from CdSe nanorods in a CdSe/P3HT/PMMA film (A and B) and in a CdSe/PMMA film (C and D). The band edge emission was recorded from 560 to 600 nm and the trap state emission was recorded at wavelengths longer than 700 nm. The images show the maximum counts across 200 video frames for each pixel. They have been background subtracted using the ImageJ software ("rolling ball" method, 50 pixel ball diameter). The relative emission rate depends on the sample, as indicated by the color scales, with the highest overall emission observed for CdSe/P3HT/PMMA. The lower panel shows histograms of the band edge (E) and trap emission(F) for the two different samples. The videos used to produce these images are included in the Supporting Information (Videos S1 and S2).

channels are anticorrelated for both the CdSe/PMMA and CdSe/P3HT/PMMA samples. That is, high signals in one emission channel are most often observed with low signals in the other channel, leading to relatively high intensity along the two axes and low intensity along the diagonal of the correlation plots in Figure 2. These results stand in strong contrast with the uncorrelated dark counts from the instrument (Figure 2A). The correlation maps indicate that nanorods typically emit into only a single channel (band edge or trap) within the 20 ms signal integration time of the dual-channel confocal measurements. In principle, switching between the two emission channels could take place over a wide range of time scales, but we conclude from the data in Figure 2 that the typical switching time must be similar to or longer than the integration time of the microscope.

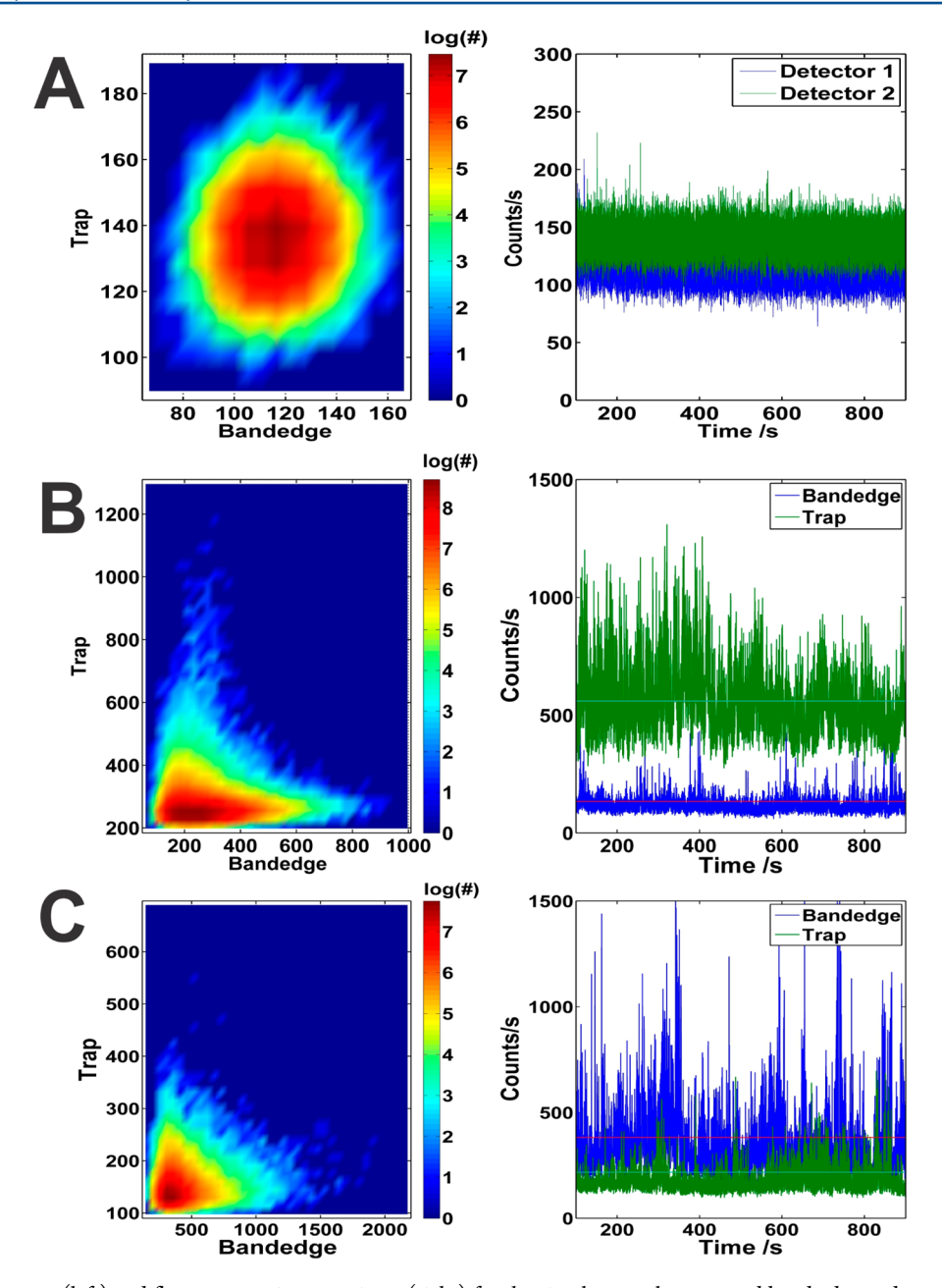


Figure 2. Correlation maps (left) and fluorescence time transients (right) for the simultaneously measured band edge and trap emission channels at a single site using confocal microscopy. The panels on the left display the population (on a natural log scale) of time bins exhibiting the count levels in each channel. The panels from top to bottom show the uncorrelated dark counts of the instrument (A), and anticorrelated CdSe nanorod emission signals for CdSe/PMMA (B) and CdSe/P3HT/PMMA (C) films. The horizontal lines appended to the time transients depict the threshold values used in calculating the correlation coefficients. The correlation coefficients are found to be -0.41 and -0.34 for the CdSe/PMMA and CdSe/P3HT/PMMA samples, respectively.

The microscopy images in Figure 1 and the single-point emission data in Figure 2 both demonstrate an increased likelihood of detecting band edge emission from the nanorods in the presence of P3HT compared with an undoped PMMA matrix. This behavior was previously attributed to static electron transfer from P3HT that fills the low-lying, unoccupied trap sites at the surface of the CdSe nanorods and in the PMMA matrix. Here, we present a quantitative analysis of the switching rates to further probe how doping the PMMA matrix with P3HT affects the millisecond-scale kinetics of band edge and trap emission from CdSe. The observation of distinct emission channels in these experiments reveals the relative switching rates among all three states of the CdSe nanorods

(i.e., band edge emission, trap emission, and dark states). The probabilities of switching between each of the three available states are reported in Table 1. The values in the table represent the relative probability that the signal will change from one particular state to another. For example, the change from band edge emission to the OFF state accounts for 24.6% of all observed transitions in the CdSe/PMMA sample, but only 21.5% of transitions for CdSe/P3HT/PMMA. The values in Table 1 are *relative* probabilities, and therefore depend on the blinking rates of the two ON states as well as the average lifetime of each state. The lifetimes were analyzed separately by fitting the distributions of ON and OFF times with a power law function,  $P(t) \propto t^{\alpha}$ . Results for the CdSe/PMMA and CdSe/

Table 1. Relative Probabilities of Switching between Trap Emission, Band Edge Emission, and OFF States in CdSe Nanorods in PMMA and P3HT/PMMA Matrices<sup>a</sup>

	CdSe/PMMA	CdSe/P3HT/PMMA	significance
band edge state → OFF state	$24.6 \pm 2.9$	$21.5 \pm 1.6$	93%
OFF state → band edge state	$24.8 \pm 2.9$	$21.6 \pm 1.6$	95%
trap state → band edge state	$1.36 \pm 0.27$	$2.25 \pm 0.28$	>99%
band edge state → trap state	$1.63 \pm 0.33$	$2.33 \pm 0.28$	>99%
trap state → OFF state	$23.9 \pm 2.8$	$26.2 \pm 1.5$	84%
OFF state → trap state	$23.7 \pm 2.8$	$26.1 \pm 1.5$	88%

<sup>&</sup>lt;sup>a</sup>Error bars depict the 95% confidence interval. Significance gives the confidence level at which the pairs of measurements differ in a t-test.

P3HT/PMMA films are summarized in Table 2, which shows that the observed lifetimes of all three states are longer (smaller  $\alpha$ ) in the presence of P3HT. <sup>22</sup>

Several conclusions can be drawn from the relative switching probability data in Table 1. First, switching from one emissive (ON) state to another almost always goes through a dark (OFF) state. In other words, transitions directly from one emitting state to another are very rare. In fact, observation of these direct transitions may simply reflect "missing" OFF states that occur within the limited time resolution of the measurement. This observation is consistent with the negative correlation of the two emissive states that was discussed above. Second, the nearly identical complementary switching probabilities (e.g., trap  $\rightarrow$  OFF and OFF  $\rightarrow$  trap) for both band edge and trap emission channels confirms that continuous irradiation does not significantly change the fluorescence behavior of the CdSe nanorods over time, for example by increasing the likelihood of one emission state over the other. Third, the inclusion of P3HT in the matrix changes the fluorescence behavior of the CdSe nanorods. Specifically, the probability of band edge  $\rightarrow$  OFF transitions decreases in the presence of P3HT, while the probability of trap  $\rightarrow$  OFF transitions increases under the same conditions. The different relative probabilities for these transitions reflects the reduced intermittency of the band edge emission state in CdSe/P3HT/ PMMA compared with CdSe/PMMA. The band edge emission blinks less in the presence of P3HT, so we observe fewer transitions into and out of this state relative to the other possible transitions. The relative probability of a transition involving the trap emission therefore increases, even though we show below that P3HT slightly reduces the blinking rate of the trap emission state. Similarly, transitions directly between the two ON states are more likely to be observed in the presence of P3HT because the reduced blinking of both states results in fewer overall transitions involving the dark state.

The lifetime data in Table 2 clearly reflects the reduced blinking of CdSe in both the band edge and trap emission channels in the presence of P3HT. In other words, the longer average ON times (smaller  $\alpha$ ) of the band edge and trap emission states are a direct consequence of reduced

Table 2. Power Law Exponents for Single CdSe Nanorod Blinking  $(t \text{ is in seconds})^a$ 

$P(t) \approx t^{\alpha}$	CdSe/PMMA	CdSe/P3HT/PMMA	significance
OFF state	$-1.19 \pm 0.07$	$-1.10 \pm 0.04$	97%
band edge state	$-1.92 \pm 0.10$	$-1.80 \pm 0.06$	96%
trap state	$-2.10 \pm 0.08$	$-1.88 \pm 0.05$	>99%

<sup>&</sup>lt;sup>a</sup>Error bars depict the 95% confidence interval. Significance gives the confidence level at which the pairs of measurements differ in a *t*-test.

intermittency in CdSe/P3HT/PMMA compared with the undoped CdSe/PMMA film. As described previously, static charge transfer from P3HT increases the relative band edge emission intensity and reduces the blinking of the band edge emission state by prefilling surface trap sites.<sup>22</sup> Finally, in addition to the longer lifetimes of the ON states, we observe slightly longer OFF times in the presence of P3HT. The longer lifetime of the OFF states may be a result of selectively filling relatively shallow surface traps via electron transfer from P3HT. Shallow traps containing the most weakly bound electrons are probably responsible for the shortest OFF times in the blinking measurements, therefore preferential filling of the shallow traps would yield a longer average OFF time. Note that the sum of the power law exponents of the ON and OFF times in the blinking experiments are not expected to be the same for the different films.

**Ultrafast Charge Transfer Dynamics.** In order to probe the interaction between P3HT and CdSe nanorods directly, we used ultrafast spectroscopy to observe the charge transfer dynamics following excitation of the conductive polymer at 630 nm. The top panel of Figure 3 shows the static absorption

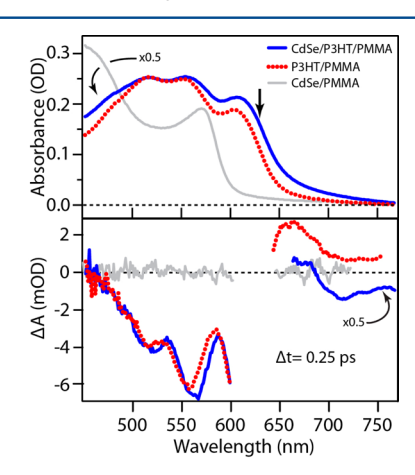


**Figure 3.** Top panel: Static absorption spectra of CdSe/PMMA, P3HT/PMMA, and CdSe/P3HT/PMMA films used in the transient absorption measurements. Bottom panel: Transient absorption spectra of all three samples at a delay of 0.25 ps following excitation at 630 nm.

spectra of the CdSe/PMMA, P3HT/PMMA, and CdSe/P3HT/PMMA films. Samples of dilute P3HT without CdSe nanorods and of nanorods without P3HT reveal the dynamics of the individual components in the PMMA matrix and provide an important reference point for comparison with the composite CdSe/P3HT/PMMA film. A strong shoulder near 620 nm in the static absorption spectra of the films containing P3HT is similar to the interchain absorption band observed in

well-ordered (e.g., crystalline) P3HT and, therefore, indicates that the conjugated polymer is highly ordered. 31,32 Importantly, this low energy transition of the structurally ordered P3HT polymer extends well below the band edge of the CdSe nanorods near 570 nm. If the P3HT were amorphous, as in liquid solutions, we would not expect to see the strong absorption near 620 nm. In fact, the relative amplitudes of the absorption at 560 and 620 nm suggest that the presence of CdSe enhances the structural order of dilute P3HT in the CdSe/P3HT/PMMA film compared with a P3HT/PMMA film in the absence of nanorods.

The bottom panel of Figure 3 shows the transient absorption spectra of all three samples following excitation at 630 nm. These experiments exclusively excite the P3HT polymer because the excitation energy is below the band gap of the CdSe nanoparticles, in contrast with the microscopy experiments, where both components are excited by the 488 nm photons. As expected, no transient absorption signal is observed for the CdSe/PMMA film, whereas excitation of the two samples containing P3HT leads to a strong transient response. Figure 4 compares the temporal evolution of the transient absorption at three different wavelengths for the P3HT/PMMA and CdSe/P3HT/PMMA films.

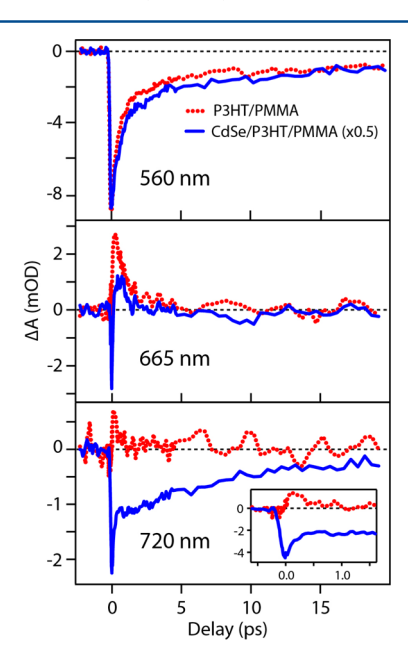


**Figure 4.** Transient absorption at 560, 665, and 720 nm as a function of delay following 630 nm excitation of P3HT/PMMA (dashed red line) and CdSe/P3HT/PMMA (solid blue line).

The transient absorption spectrum of the P3HT/PMMA film at 0.25 ps has two main features, a negative band in the 475–600 nm range and a positive band in the 650–765 nm region. The negative signal resembles the inverse of the static P3HT absorption spectrum and appears within the instrument response time. We assign this feature as the ground state bleach of the conductive polymer. The positive signal in the region near 665 nm appears on a time scale that is slightly longer than the instrument response, and then decays with an exponential time constant of about 1 ps. This transient absorption signal closely resembles the behavior of an excited state absorption band that was previously reported in the same wavelength range for crystalline films of P3HT.<sup>33</sup> The dynamics

of the P3HT/PMMA film are therefore consistent with the observation from the static spectrum that the P3HT conductive polymer aggregates into well-ordered, crystalline microdomains within the PMMA matrix.

The transient absorption spectrum of the CdSe/P3HT/ PMMA film is similar to that of the P3HT/PMMA film, except for additional negative contributions in the range 550-580 nm and above ~675 nm. We assign the new negative signal in the long-wavelength region of the spectrum as stimulated emission from the conduction band of CdSe to unoccupied defect sites located above the valence band. This assignment is consistent with the trap emission spectrum of etched CdSe nanorods in solution (see below). The instrument-limited rise of the stimulated emission signal is a clear sign of ultrafast electron transfer from the initially excited P3HT to the CdSe nanorods, because there can be no emission from CdSe without first creating an excitation in the nanoparticle. Furthermore, the electron must radiatively recombine with a trapped hole lying above the valence band, because the valence band of the nanoparticle remains fully occupied following excitation at 630 nm. Thus, the ultrafast measurement confirms that the belowband edge trap emission observed under 488 nm excitation in the microscopy experiments is a result of radiative relaxation of a conduction band electron to a defect site lying above the valence band.

The bottom panel of Figure 4 shows the temporal evolution of the stimulated emission band at 720 nm, where there is only a minimal contribution from the positive P3HT excited-state absorption. The signal at 720 nm reveals the relative population of charge carriers in the CdSe conduction band as a function of time. An instrument-limited appearance of the emission signal indicates that the charge transfer from P3HT to the CdSe nanorods occurs within the ~140 fs time resolution of our experiment. This ultrafast charge transfer confirms that there is strong coupling between P3HT and the CdSe nanoparticles. The emission decays with sub-picosecond and few-picosecond time scales, suggesting two decay pathways.34 Rapid nonradiative recombination of the charge-transfer excitation is consistent with the observation of very weak nanorod emission in widefield microscopy images that were obtained with 632 nm excitation. The decay rates provide a direct measure of the interfacial charge carrier dynamics following excitation of

The transient absorption signal in the region of the P3HT ground-state bleach provides additional evidence for charge transfer from P3HT to the CdSe nanorods. Although scattering of the pump light obscures the transient spectra in the range 600-650 nm, the bottom panel of Figure 3 shows that the negative feature in the P3HT ground-state bleach near 550 nm shifts to longer wavelength by about 10 nm in the CdSe/ P3HT/PMMA sample. Placing an electron in the conduction band of CdSe blocks a possible transition from the valence band, and results in a negative feature in the transient absorption spectrum (at the ~565 nm band edge) due to Pauli blocking. The negative signal in the CdSe/P3HT/PMMA sample therefore reports on both the ground-state bleach of P3HT and the conduction band charging of CdSe. Consistent with the above description of the charge transfer dynamics, the additional bleaching at the CdSe band edge decays on the same time scale as the stimulated emission at 720 nm (see Figure 4).

Role of Photoetching. Trap emission from the CdSe nanorods can be related to the chemical composition (e.g., defects) at the nanoparticle surface. In the case of a cadmium

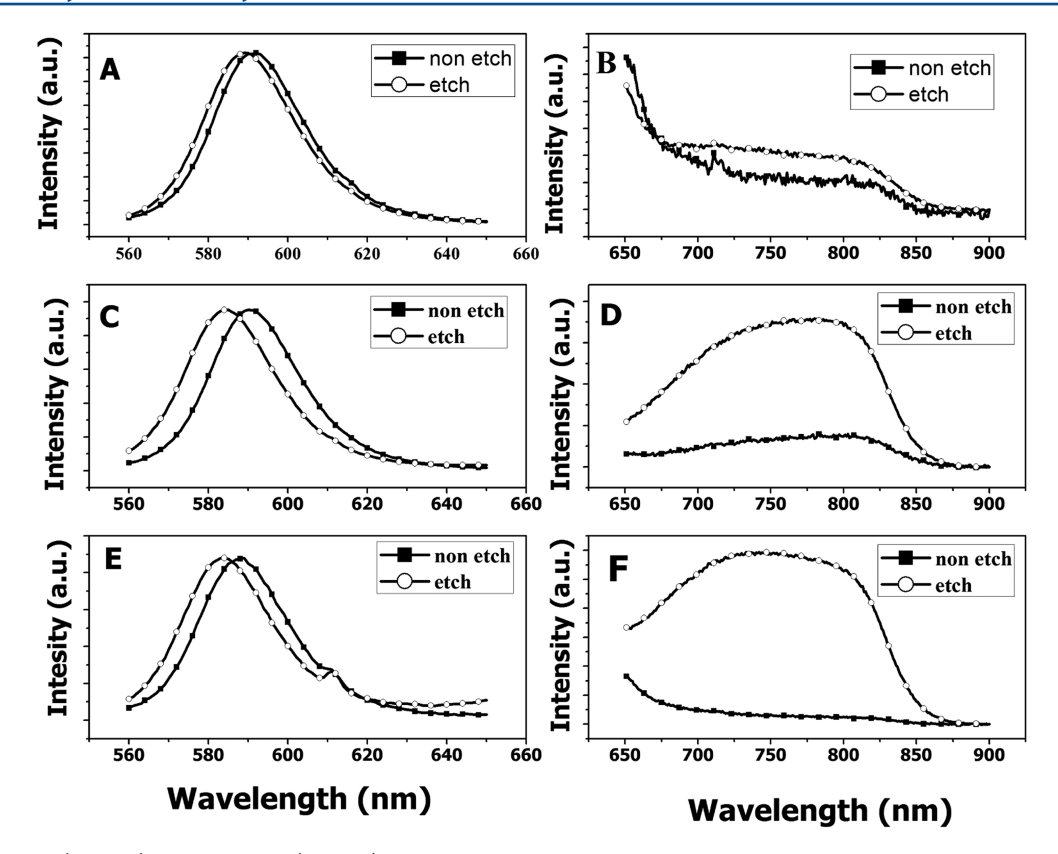


**Figure 5.** Band edge (A, C, E) and trap state (B, D, F) emission of CdSe nanorods before and after etching treatment. Non etched and etched nanorods are represented as filled squares and hollow circles respectively. Nanorods in toluene are shown in panels A and B. An equal mixture of toluene and chloroform with nanorods is shown in panels C and D. An equal mixture of toluene and chloroform with nanorods and PMMA is shown in panels E and F. The spectra are normalized to the maximum of the band edge emission.

rich surface, Knowles et al.<sup>23</sup> observed the radiative recombination of delocalized conduction band electrons with trapped holes. Those authors point out that there are several emissive excitonic states present where the hole is not in its initial delocalized state. Kalyuzhny and Murray similarly showed that strongly bound triocytylphospine ligands enhance the red-shifted emission associated with traps by preferentially binding Se atoms at the surface of CdSe nanoparticles, effectively leaving the particles with a cadmium rich surface.<sup>24</sup> Both of these previous observations are important because they provide insight into the possible structural origin of the trap emission observed in the present experiments.

It has been shown in the literature that either chemical or photochemical etching of CdSe can occur in the presence of chlorinated solvents.<sup>35</sup> Therefore, we propose that exposure to chloroform during film preparation creates surface defects in the CdSe nanorods that are responsible for strong trap emission in the CdSe/polymer samples. To test this hypothesis, we observed the fluorescence spectrum of CdSe nanorods that were dissolved in various solvents and then heated at 40 °C for 72 h under continuous irradiation at 405 nm. The solutions included CdSe nanorods dissolved in either toluene (Figure 5A and B), a mixture of equal portions of toluene and chloroform (Figure 5C and D), or a toluene-chloroform mixture with added PMMA (Figure 5E and 5F). The left and right panels of Figure 5 show the normalized band edge and trap emission spectra, respectively. The trap emission intensity increased substantially in the chloroform-containing solutions, both in absolute terms and relative to the band edge emission of the CdSe nanorods.

Transmission electron microscopy (TEM) images of the nanorods before and after etching show that the nanorods become shorter in length, while their diameters change very little. The length of the CdSe nanorods were reduced by 34% while the diameter decreased by only 4%. The shift of the band edge emission to shorter wavelength for the etched nanorods in Figure 5 is consistent with the reduced Stokes shift with decreasing aspect ratio that was previously observed for CdSe nanorods. Thus, the TEM and fluorescence measurements confirm that etching in the presence of chloroform removes atoms from the ends of the CdSe nanorods.<sup>35</sup> It seems likely that this etching process produces the defect sites at the CdSe surface that are responsible for trap emission in our experiments. The defects probably represent a cadmium rich surface, based on earlier observations of trap emission from CdSe nanocrystals that were explained by the preferential binding of Se atoms with strongly coordinating triocytylphospine, which reduces the cadmium-selenium interaction and leaves a cadmium rich nanoparticle surface.<sup>24</sup> In the previous work it was also observed that the trap emission gets stronger over time when the nanoparticles are exposed to light, suggesting that photochemical etching also occurs in the presence of residual chloroform from solution processing of the nanorods. In our experiments, trap state emission became stronger with extended illumination of both the PMMAcontaining solution and film samples. This effect was less pronounced when P3HT was added to the PMMA film.<sup>22</sup>

Model for Band Edge and Trap Emission Dynamics. The excited state dynamics of dispersed CdSe nanorods in CdSe/PMMA and CdSe/P3HT/PMMA films have been

#### Model for defect filling **CdSe** excitation **P3HT** excitation Р3Н CdSe Rod **Р3НТ** CdSe Rod CdSe Rod CB CB Stimulated Bleach Trap Emission Surface Surface defects defects

Figure 6. Simplified scheme for the interaction between CdSe nanorods and P3HT in the fluorescence blinking and the transient absorption experiments.

explored by both ms-scale fluorescence microscopy and fs-scale transient absorption spectroscopy. These two experimental tools probe the dynamics on very different time scales, using different excitation wavelengths. Furthermore, the ultrafast experiments probe the average properties of P3HT and CdSe nanorods in the films, while the microscopy experiments provide data at the level of single nanoparticles. Nevertheless, these experiments provide complementary information about the charge carrier dynamics and emission properties of hybrid CdSe/polymer films, including the important role of charge transfer between P3HT and the CdSe nanorods. Figure 6 summarizes a few of the key processes underlying the dynamics of these systems.

The left panel of Figure 6 depicts a static charge transfer process that pacifies the CdSe/polymer interface by filling surface defect sites. The etching experiments described above indicate that at least some of the surface defects are likely caused by chemical or photochemical etching of the nanorods through exposure to chloroform during film preparation, which leads to an excess of cadmium atoms at the surface of the nanoparticle. The center panel illustrates the competing emission channels following direct optical excitation of the etched CdSe nanorod. Importantly, electrons excited to the conduction band can radiatively relax into either the valence band or intraband surface defects. These two emission channels are responsible for the two possible emission states identified in our microscopy measurements. The observed negative correlation of the band edge emission and trap emission states in the confocal microscopy measurements indicates that an individual nanorod preferentially emits into only a single channel over a period of many milliseconds to seconds under continuous irradiation. In other words, each nanoparticle may cycle many times before changing emission channels. Within a single emission channel, however, individual nanoparticles experience fluorescence intermittency (or blinking) with a distribution of ON times that follows a power law. The dark (OFF) states in which the nanoparticle does not emit light into either channel are a result of charge trapping that temporarily leaves the nanoparticle in a nonequilibrium state that is unfavorable for emission.

As noted above, the addition of dilute P3HT to the CdSe/PMMA film increases the band edge emission intensity of the nanorods (see Figure 1). Static charge transfer from P3HT into the otherwise unoccupied trap states blocks the longer-wavelength emission channel, and therefore favors emission at the band edge.<sup>22</sup> Importantly, the observation of trap emission even in the presence of P3HT suggests that at least some of the trap states remain unoccupied. In addition to incomplete filling (i.e., limited reducing capacity of the P3HT),

trapped electrons can rapidly relax to repopulate new holes created in the valence band by nanorod excitation. Traps that are long-lived probably contribute to fluorescence intermittency by blocking further excitation and emission processes in the nanorod.

The fluorescence intermittency experiments show that P3HT also impacts the blinking dynamics of the CdSe nanorods. Analysis of fluorescence time transients obtained from single sites (i.e., single nanorods) using a power law model demonstrates that the ON times for both band edge and trap emission become longer, on average, in the presence of P3HT. Furthermore, analysis of the probabilities of switching between the two ON states and the OFF state reveals that the probability of a transition from band edge emission to the OFF state is lower in the presence of P3HT. These observations are consistent with the filling of defects (traps in both the CdSe and the matrix)<sup>37</sup> by electrons from P3HT. On the whole, these observations and conclusions explain the enhancement of CdSe nanorod band edge emission observed in both the confocal and widefield image data (see Figures 1 and 2, and the videos presented in the Supporting Information). The microscopy experiments reveal that the switching among trap emission, band edge emission, and dark (OFF) states is slow compared to the signal integration time (20 ms). The slow dynamic switching between the trap and band edge emission in fluorescence blinking experiments allows us to assign the time scale of charge trapping as a few milliseconds.

Finally, the right panel in Figure 6 illustrates the electron transfer process that occurs following optical excitation of P3HT in the presence of a CdSe nanorod. The ultrafast transient absorption measurements show conclusively that an electron is transferred to the conduction band of the nanoparticle within the 140 fs time resolution of the measurement. The charge-transfer excited state decays with subps and few-ps time scales. Trap emission is not observed in fluorescence microscopy measurements using a 632 nm excitation, consistent with the very short lifetime of the charge-transfer state. Unlike direct excitation of a CdSe nanorod, the charge-transfer state created by excitation of P3HT and subsequent electron transfer to the nanoparticle does not produce a hole in the CdSe valence band, therefore the only possibly emission channel is to the intraband defect sites. The ultrafast transient absorption measurements therefore provide strong support for the above model for trap emission by confirming the presence of the trap states, their position above the valence band, their participation in radiative relaxation of excited nanorods, and even the role played by charge transfer in modulating their population.

# CONCLUSIONS

Trap states play an important role in the conversion of photon energy into electricity in solar cells. The combination of ultrafast spectroscopy and emission-state resolved fluorescence microscopy experiments reported here provides a unique opportunity to observe the dynamics of the emitting states on very different time scales. Specifically, the role of the trap state emission of CdSe nanorods is investigated in CdSe/ PMMA and CdSe/P3HT/PMMA blend films. Transient absorption measurements that directly excite P3HT (below the band edge of CdSe) reveal ultrafast electron transfer from the photoexcited P3HT to the CdSe nanorods, resulting in a transient signal in the 630-780 nm range that is assigned as stimulated emission from the conduction band of CdSe to defect (trap) states above the valence band. The fluorescence microscopy measurements monitor emission under continuous irradiation at 488 nm, which excites both CdSe nanorods and the P3HT polymer. In the literature, trap states of CdSe nanocrystals are mostly categorized as nonemissive states, but we find that chemical etching creates emissive trap states that are distinct from the band edge emission state. The emissive trap states are a direct result of chemical etching by the chlorinated solvent used to fabricate the films.

#### ASSOCIATED CONTENT

### **S** Supporting Information

Additional spectroscopic data, images, and videos for CdSe nanorods dispersed in PMMA and dilute P3HT/PMMA films along with background data from PMMA and dilute P3HT/PMMA films in the absence of CdSe nanorods. This material is available free of charge via the Internet at http://pubs.acs.org.

### AUTHOR INFORMATION

### **Corresponding Authors**

- \*E-mail: higgins@ksu.edu (D.A.H.).
- \*E-mail: elles@ku.edu (C.G.E.).
- \*E-mail: chikan@ksu.edu (V.C.).

#### Notes

The authors declare no competing financial interest.

### ACKNOWLEDGMENTS

This work was supported by the National Science Foundation (No. EPS-0903806). Takashi Ito is thanked for providing access to the spectroscopic ellipsometer. J.M.W. is supported by the Madison and Lila Self Graduate Fellowship Program at the University of Kansas. C.G.E is grateful for additional support from a NSF Career Award (CHE-1151555). The widefield microscope was provided through funding from the Division of Chemical Sciences, Geosciences, and Biosciences, Office of Basic Energy Sciences of the U.S. Department of Energy (DE-FG02-09ER16095).

# **■** REFERENCES

- (1) Dayal, S.; Reese, M. O.; Ferguson, A. J.; Ginley, D. S.; Rumbles, G.; Kopidakis, N. The Effect of Nanoparticle Shape on the Photocarrier Dynamics and Photovoltaic Device Performance of Poly(3-Hexylthiophene):Cdse Nanoparticle Bulk Heterojunction Solar Cells. *Adv. Funct. Mater.* **2010**, *20*, 2629–2635.
- (2) Goodman, M. D.; Xu, J.; Wang, J.; Lin, Z. Q. Semiconductor Conjugated Polymer-Quantum Dot Nanocomposites at the Air/Water Interface and Their Photovoltaic Performance. *Chem. Mater.* **2009**, *21*, 934–938.

- (3) Zhai, G.; Church, C. P.; Breeze, A. J.; Zhang, D.; Alers, G. B.; Carter, S. A. Quantum Dot Pbs(0.9)Se(0.1)/Tio(2) Heterojunction Solar Cells. *Nanotechnology* **2012**, *23*, 405401.
- (4) Nam, M.; Kim, S.; Kang, M.; Kim, S. W.; Lee, K. K. Efficiency Enhancement in Organic Solar Cells by Configuring Hybrid Interfaces with Narrow Bandgap Pbsse Nanocrystals. *Org. Electron.* **2012**, *13*, 1546–1552.
- (5) Saunders, B. R.; Turner, M. L. Nanoparticle-Polymer Photovoltaic Cells. *Adv. Colloid Interface Sci.* **2008**, *138*, 1–23.
- (6) Greenham, N. C.; Peng, X.; Alivisatos, A. P. Charge Separation and Transport in Conjugated-Polymer/Semiconductor-Nanocrystal Composites Studied by Photoluminescence Quenching and Photoconductivity. *Phys. Rev. B: Condens. Matter Mater. Phys* **1996**, *54*, 17628
- (7) Padilha, L. A.; Stewart, J. T.; Sandberg, R. L.; Bae, W. K.; Koh, W.-K.; Pietryga, J. M.; Klimov, V. I. Aspect Ratio Dependence of Auger Recombination and Carrier Multiplication in Pbse Nanorods. *Nano Lett.* **2013**, *13*, 1092–1099.
- (8) Ip, A. H.; Thon, S. M.; Hoogland, S.; Voznyy, O.; Zhitomirsky, D.; Debnath, R.; Levina, L.; Rollny, L. R.; Carey, G. H.; Fischer, A.; et al. Hybrid Passivated Colloidal Quantum Dot Solids. *Nat. Nanotechnol.* **2012**, *7*, 577–582.
- (9) Zhao, L.; Lin, Z. Q. Crafting Semiconductor Organic-Inorganic Nanocomposites Via Placing Conjugated Polymers in Intimate Contact with Nanocrystals for Hybrid Solar Cells. *Adv. Mater.* (Weinheim, Ger.) 2012, 24, 4353–4368.
- (10) Hohng, S.; Ha, T. Near-Complete Suppression of Quantum Dot Blinking in Ambient Conditions. *J. Am. Chem. Soc.* **2004**, *126*, 1324–1325
- (11) Krauss, T. D.; Brus, L. E. Charge, Polarizability, and Photoionization of Single Semiconductor Nanocrystals. *Phys. Rev. Lett.* **1999**, 83, 4840–4843.
- (12) Kuno, M.; Fromm, D. P.; Hamann, H. F.; Gallagher, A.; Nesbitt, D. J. Nonexponential "Blinking" Kinetics of Single Cdse Quantum Dots: A Universal Power Law Behavior. *J. Chem. Phys.* **2000**, *112*, 3117–3120.
- (13) Mahler, B.; Spinicelli, P.; Buil, S.; Quelin, X.; Hermier, J.-P.; Dubertret, B. Towards Non-Blinking Colloidal Quantum Dots. *Nat. Mater.* **2008**, *7*, 659–664.
- (14) Shimizu, K. T.; Neuhauser, R. G.; Leatherdale, C. A.; Empedocles, S. A.; Woo, W. K.; Bawendi, M. G. Blinking Statistics in Single Semiconductor Nanocrystal Quantum Dots. *Phys. Rev. B: Condens. Matter Mater. Phys.* **2001**, *63*, 205316.
- (15) Wang, S.; Querner, C.; Emmons, T.; Drndic, M.; Crouch, C. H. Fluorescence Blinking Statistics from Cdse Core and Core/Shell Nanorods. *J. Phys. Chem. B* **2006**, *110*, 23221–23227.
- (16) Knappenberger, K. L., Jr.; Wong, D. B.; Xu, W.; Schwartzberg, A. M.; Wolcott, A.; Zhang, J. Z.; Leone, S. R. Excitation-Wavelength Dependence of Fluorescence Intermittency in Cdse Nanorods. *ACS Nano* 2008, 2, 2143–2153.
- (17) Galland, C.; Ghosh, Y.; Steinbruck, A.; Sykora, M.; Hollingsworth, J. A.; Klimov, V. I.; Htoon, H. Two Types of Luminescence Blinking Revealed by Spectroelectrochemistry of Single Quantum Dots. *Nature* **2011**, *479*, 203–207.
- (18) Li, S.; Steigerwald, M. L.; Brus, L. E. Surface States in the Photoionization of High-Quality Cdse Core/Shell Nanocrystals. *ACS Nano* **2009**, *3*, 1267–1273.
- (19) Mokari, T.; Banin, U. Synthesis and Properties of Cdse/Zns Core/Shell Nanorods. *Chem. Mater.* **2003**, *15*, 3955–3960.
- (20) Jha, P. P.; Guyot-Sionnest, P. Trion Decay in Colloidal Quantum Dots. ACS Nano 2009, 3, 1011–1015.
- (21) Jander, S.; Kornowski, A.; Weller, H. Energy Transfer from Cdse/Cds Nanorods to Amorphous Carbon. *Nano Lett.* **2011**, *11*, 5179–5183.
- (22) Roy, S.; Aguirre, A.; Higgins, D. A.; Chikan, V. Investigation of Charge Transfer Interactions in Cdse Nanorod P3ht/Pmma Blends by Optical Microscopy. *J. Phys. Chem. C* **2012**, *116*, 3153–3160.

- (23) Knowles, K. E.; McArthur, E. A.; Weiss, E. A. A Multi-Timescale Map of Radiative and Nonradiative Decay Pathways for Excitons in Cdse Quantum Dots. *ACS Nano* **2011**, *5*, 2026–2035.
- (24) Kalyuzhny, G.; Murray, R. W. Ligand Effects on Optical Properties of Cdse Nanocrystals. *J. Phys. Chem. B* **2005**, *109*, 7012–7021.
- (25) Gomez-Campos, F. M.; Califano, M. Hole Surface Trapping in Cdse Nanocrystals: Dynamics, Rate Fluctuations, and Implications for Blinking. *Nano Lett.* **2012**, *12*, 4508–4517.
- (26) Puzder, A.; Williamson, A. J.; Zaitseva, N.; Galli, G.; Manna, L.; Alivisatos, A. P. The Effect of Organic Ligand Binding on the Growth of Cdse Nanoparticles Probed by Ab Initio Calculations. *Nano Lett.* **2004**, *4*, 2361–2365.
- (27) Wang, H. M.; Bardo, A. M.; Collinson, M. M.; Higgins, D. A. Microheterogeneity in Dye-Doped Silicate and Polymer Films. *J. Phys. Chem. B* **1998**, *102*, 7231–7237.
- (28) Tran, Ba, K. H.; Everett, T. A.; Ito, T.; Higgins, D. A. Trajectory Angle Determination in One Dimensional Single Molecule Tracking Data by Orthogonal Regression Analysis. *Phys. Chem. Chem. Phys.* **2011**, *13*, 1827–35.
- (29) Giblin, J.; Syed, M.; Banning, M. T.; Kuno, M.; Hartland, G. Experimental Determination of Single Cdse Nanowire Absorption Cross Sections through Photothermal Imaging. *ACS Nano* **2010**, *4*, 358–364.
- (30) These lifetimes refer to the average residence time in any one of the ON or OFF states, rather than the time spent in a particular emission channel inclusive of blinking.
- (31) Sirringhaus, H.; Brown, P. J.; Friend, R. H.; Nielsen, M. M.; Bechgaard, K.; Langeveld-Voss, B. M. W.; Spiering, A. J. H.; Janssen, R. A. J.; Meijer, E. W.; Herwig, P.; et al. Two-Dimensional Charge Transport in Self-Organized, High-Mobility Conjugated Polymers. *Nature* 1999, 401, 685–688.
- (32) Brown, P. J.; Thomas, D. S.; Kohler, A.; Wilson, J. S.; Kim, J. S.; Ramsdale, C. M.; Sirringhaus, H.; Friend, R. H., Effect of Interchain Interactions on the Absorption and Emission of Poly(3-Hexylthiophene). *Phys. Rev. B: Condens. Matter Mater. Phys.* **2003**, *67*.
- (33) Guo, J. M.; Ohkita, H.; Benten, H.; Ito, S. Near-Ir Femtosecond Transient Absorption Spectroscopy of Ultrafast Polaron and Triplet Exciton Formation in Polythiophene Films with Different Regioregularities. *J. Am. Chem. Soc.* **2009**, *131*, 16869–16880.
- (34) Carey, C. R.; Yu, Y.; Kuno, M.; Hartland, G. V. Ultrafast Transient Absorption Measurements of Charge Carrier Dynamics in Single Ii-Vi Nanowires. *J. Phys. Chem. C* **2009**, *113*, 19077–19081.
- (35) Lim, S. J.; Kim, W.; Jung, S.; Seo, J.; Shin, S. K. Anisotropic Etching of Semiconductor Nanocrystals. *Chem. Mater.* **2011**, 23, 5029–5036.
- (36) Hu, J. T.; Li, L. S.; Yang, W. D.; Manna, L.; Wang, L. W.; Alivisatos, A. P. Linearly Polarized Emission from Colloidal Semi-conductor Quantum Rods. *Science* **2001**, *292*, 2060–2063.
- (37) Schwartz, O.; Oron, D. A Present Understanding of Colloidal Quantum Dot Blinking. *Isr. J. Chem.* **2012**, *52*, 992–1001.